Supplementary information, figures, and tables

"High-resolution estimates of Nubia-Somalia plate motion since 20 Ma from reconstructions of the Southwest Indian Ridge, Red Sea, and Gulf of Aden"

by C. DeMets & S. Merkouriev

Overview

This supplemental document includes information and figures that are referred to within or are relevant to the main document. Much of the supplement gives an extensive description of the probabilistic methodology, assumptions, and results for estimating Nubia-Arabia plate motion across the Red Sea during the past 20 Myr.

I. Has Nubia-Somalia motion changed since 3 Ma?

In Section 3.2.1 of the main document, we describe a 10-30 $^\circ$ systematic difference between the Nubia-Somalia directions estimated using our 3.6-Myr-to-present angular velocities from Table 2 and directions determined independently from geodetic, seismologic, and geologic observations. Although this difference could indicate that the Nubia-Somalia plate slip direction has changed during the past 780,000 yrs, we instead suspect that it is an artifact of small errors in estimates of seafloor spreading rates from the Southwest Indian Ridge.

Two lines of evidence argue against the possibility that a recent change in the location of the Nubia-Somalia pole is responsible for the difference between the directions that are predicted by our new stage rotations and those estimated from geodetic and structural data. First, a significant recent change in the pole location might reasonably be expected to be accompanied by a change in the rate of motion between the two plates at most or all locations along their boundary. Instead, the Nubia-Somalia rate at the northern end of the East Africa Rift has remained steady for the past 5.2 Myr (see below). Second, the directions predicted by our new sequence of Nubia-Somalia angular velocities have not changed significantly during the past 3.6 Myr (Fig. 3b in the main document). A 10-30 $^\circ$ anticlockwise rotation of the Nubia-Somalia opening direction would thus had to have occurred within the past 0.78 Myr.

Although the arguments in the previous paragraph weigh against, but do not exclude a possible change in Nubia-Somalia motion since 3.6 Ma, we prefer an alternative, simpler explanation, namely, that the discrepancy described above is an artifact of small errors in the DeMets *et al.* (2015) estimates of seafloor spreading rates along the Southwest Indian Ridge. A Nubia-Antarctic-Somalia linear velocity triangle at the location of the Main Ethiopian Rift illustrates the basis for this argument (Fig. S1b). By inspection, the orientation of the Nubia-Somalia leg of the closed velocity triangle is sensitive to the relative lengths (rates) of the Nubia-Antarctic and Somalia-Antarctic velocities, such that small changes in the lengths of one or both of the latter two legs of the triangle cause large changes in the orientation of the former leg. Fig. S1d quantifies the trade-off; a change in the Somalia-Antarctic rate of only 1 mm yr^{-1} causes the predicted Nubia-Somalia direction to change by 10-12 $^\circ$ (red line in Fig. S1d). Via the symmetry of the velocity triangle, changes in the Nubia-Antarctic rates (or changes in the relative lengths of the Nubia-Antarctic and Somalia-Antarctic velocity vectors) have nearly the same effect (not shown).

In contrast to the above, estimates of the rate of Nubia-Somalia plate motion change by no more

than a few-tenths of a mm yr^{-1} in response to changes as large as 1.5 mm yr^{-1} in the Somalia-Antarctic rate (Fig. S1d). Via the symmetry of the velocity triangle, Nubia-Somalia plate rates are also equally insensitive to changes in Nubia-Antarctica opening rates (not shown). Nubia-Somalia plate rates that are estimated via closure of the Nubia-Antarctic-Somalia plate circuit are thus robust with respect to small errors in the DMS15 estimates of Southwest Indian Ridge seafloor spreading rates.

We conclude that errors as small as 1 mm yr^{-1} in the DMS15 estimates of recent seafloor spreading rates across the Southwest Indian Ridge may cause most or all of the discrepancy between Nubia-Somalia directions that are predicted by our new rotations and those estimated from the independent observations described above. For this reason, we place little emphasis in the main document on the time evolution of Nubia-Somalia directions and instead focus on the implications of the more robust Nubia-Somalia rates that are predicted by our rotations.

II. Arabia-Nubia rotations

Estimating Nubia-Arabia rotations that describe opening of the Red Sea during the past 20 Myr is challenging due to factors that include an absence of easily interpreted Red Sea magnetic anomalies older than $\sim$5 Ma, uncertainties in the opening age of the Red Sea, uncertainties about the pole and angle that best close the Red Sea, and uncertainty about if and when motion between Nubia and Arabia may have changed since the Red Sea opened. Divergence between the two plates has been accommodated by a combination of diking and normal faulting of the Red Sea's wide, shallow margins (Bosworth *et al.* 2005; Lazar *et al.* 2012; Almaki *et al.* 2014), seafloor spreading within the Red Sea's narrow axial trough during the past $\approx$5 Myr (Roeser 1975; Izzeldin 1987; Chu & Gordon 1998, 1999), and possible seafloor spreading before 5 Ma outside the trough (Dyment *et al.* 2013; Tapponnier *et al.* 2013).

Rotations that describe motion between Nubia and Arabia are primarily limited to geodetic angular velocities that describe their present-day motion (*e.g.* Reilinger *et al.* 2006; ArRajehi *et al.* 2010), angular velocities based on inversions of magnetic anomaly 2A (2.58-3.59 Ma) (*e.g.* Chu & Gordon 1999; DeMets *et al.* 2010), and numerous poles and angles that reconstruct the total opening of the Red Sea (references given below). The dearth of reliable kinematic information, particularly for times before $\approx$3 Ma, poses a major challenge to efforts to estimate Nubia-Somalia rotations via closure of the Nubia-Arabia-Somalia plate circuit (*e.g.* Iaffaldano *et al.* 2014*a*).

Below, we describe a probabilistic method for identifying the full range of Nubia-Arabia plate kinematic models that satisfy well-determined GPS constraints on Nubia-Arabia plate motion and also obey broad constraints on the age and opening history of the Red Sea and the associated offsets of the Dead Sea Fault and normal faults in the Gulf of Suez (Garfunkel & Beyth 2006). We assume that divergence between Nubia and Arabia has been continuous and has changed no more than once since the opening of the Red Sea. Although more complex kinematic histories are certainly possible (*e.g.* Le Pichon & Gaulier 1988), we are unconvinced that the available data warrant models more complex than a two-stage opening history.

IIa. Arabia-Nubia opening constraints and probability density functions

Eight parameters define our continuous, two-stage model for motion between Nubia and Arabia. One stage pole and stage angle specifies the displacements during the youngest (most recent) period of motion. We fix these three parameters to predefined values that are described below. A second pole and angle describe the plate displacement during the oldest of the two stages. The

final two parameters are the uncertain opening age of the Red Sea and unknown time at which Nubia-Arabia plate motion changed. The latter five parameters are varied within bounds that are prescribed by probability density functions described below.

Candidates for the pole and angular rotation rate that best describe Nubia-Arabia plate motion during geologically recent times include the 3-Myr-average angular velocity from the MORVEL global plate motion model (DeMets *et al.* 2010) or an angular velocity determined from GPS measurements. The GPS-derived, Nubia-Arabia angular velocity of Reilinger *et al.* (2006) agrees well with the MORVEL estimate, suggesting that Nubia-Arabia plate motion has been steady during the past few Myr. The more recent GPS estimate of ArRajehi *et al.* (2010) predicts motion $\sim$1 mm yr^{-1} slower than the MORVEL and Reilinger *et al.* angular velocities, but is based on more GPS stations with longer time series, particularly for the Arabia plate, than the earlier GPS estimate. We thus elected to fix the angular velocity for the youngest interval to more recent ArRajehi *et al.*'s GPS-derived angular velocity of 31.7 °N, 24.6 °E, 0.369 ° Myr^{-1}. In two cases described in the main document, we evaluated the consequences of adopting the Reiler *et al.* (2006) GPS estimate.

Probability density functions (PDF), which specify the relative likelihood that a variable will have a given value, are used to enforce geologically plausible bounds on the total opening pole and angle for the Red Sea, the opening age of the Red Sea, and the age at which Nubia-Arabia plate motion changed. These are described next.

Probability density function for the Red Sea opening age: Bosworth *et al.* (2005) and Reilinger *et al.* (2006) propose that opening of the Red Sea commenced at $\sim$24 Ma, when volcanism and rift-normal extensional faulting initiated nearly synchronously along the whole length of the Red Sea. The ages of volcanic rocks that mark this possible initial phase of Red Sea opening range from $\sim$25 Ma to 22 Ma (Bosworth *et al.* 2005). Structural and radiometric studies of volcanic rocks along the southern Red Sea margin in Ethiopia suggest that opening there may have started as early as 29-26 Ma (Wolfenden *et al.* 2005). For our analysis, we elected to constrain the opening age of the Red Sea via a Gaussian probability distribution with a mean opening age of 24 Myr, a 1σ limit of $\pm$1 Myr (Fig. S2h), and absolute upper and lower cut-off ages of 26 Ma and 22 Ma. We explored but do not discuss solutions with assumed opening ages as early as 30 Ma, which differ only marginally from the results described below and in the main document.

PDF for the age of a change in motion: In the absence of a complete Red Sea magnetic reversal sequence, previous authors have inferred when changes in Nubia-Arabia plate motion may have occurred. These include proposed changes at 4.7 Ma (Le Pichon & Gaulier 1988), 13 Ma (Le Pichon & Gaulier 1988; ArRajehi *et al.* 2010), and $\sim$18 Ma (Garfunkel & Beyth 2006). A significant change in Nubia-Arabia plate motion at 4.7 Ma seems unlikely given that kinematic studies of the seafloor spreading centers that surround Africa have not uncovered any evidence for a significant change in the motion of the Nubia or Somalia plates during the past 6 Myr (Merkouriev & DeMets 2006; Fournier *et al.* 2010; Merkouriev & DeMets 2014; DeMets, Iaffaldano, & Merkouriev, 2015; DeMets, Merkouriev, & Sauter 2015).

For the analysis below, we adopt broad limits of 18 Ma to 6 Ma for a possible change in Nubia-Arabia motion, thereby including nearly the entire range of times proposed in the literature. We adopt a non-prejudicial approach to when motion may have changed and thus define the probability that motion changed at any given time between 18 and 6 Ma to be equal. The resulting equal-probability PDF is shown in Fig. S2g.

Total opening rotation PDFs: We account for the uncertainty in the total Red Sea opening rotation on two levels. At the broadest level, we explore solutions that are based on six different published estimates of the Red Sea's total opening rotation. Two of these rotations were derived by the original authors so as to reconstruct the Red Sea's present coastlines onto each other (McKenzie

et al. 1970; Sultan *et al.* 1992, 1993), but use different approaches and assumptions for aligning distinctive geologic features that are found on both margins of the Red Sea. Both sets of authors assume that the Red Sea is underlain by oceanic lithosphere and thus do not correct their rotations for likely thinning of the continental crust beneath the Red Sea. Consequently, both rotations maximize the total movement between Nubia and Arabia. Neither of these rotations was adjusted by their authors to satisfy geometric constraints that are imposed by the observed offset of the Dead Sea Fault and opening estimated across the Gulf of Suez.

The other four rotations used here were estimated by Joffe & Garfunkel (1987), Le Pichon & Gaulier (1988), and Garfunkel & Beyth (2006) (rotations Rt2 and Rt3 in their Table 3). All four rotations include adjustments to their opening angles and poles to compensate for modest stretching of the continental crust beneath the Red Sea. All four are also tailored to satisfy geometric constraints that are imposed by the observed 105-km lateral offset of the Dead Sea Fault and opening estimated across the Gulf of Suez. They thus sample a range of geologically plausible solutions that differ distinctly from those of McKenzie *et al.* (1970) and Sultan *et al.* (1992, 1993).

We did not explore rotations that were derived presuming that the Red Sea is underlain by large amounts of thinned continental lithosphere (*e.g.* Le Pichon & Francheteau 1978; Izzeldin 1987) because such models are in conflict with more recent evidence that much of the central Red Sea is underlain by oceanic lithosphere or heavily intruded continental lithosphere (Mitchell & Park 2014).

Near the midpoint of the Red Sea (20 °N, 38 °E), the six solutions listed above predict total opening of the Red Sea that ranges from 240 km to 290 km. The ≈50-km range in the estimated opening distances, which reflects the differing approaches and assumptions that are used by the authors for their reconstructions, bracket the likely minimum and maximum estimates of the opening of the Red Sea and also sample a range of possible opening directions. All six are used below in order to fully explore how uncertainties in Nubia-Arabia reconstructions propagate into estimates of the uncertainties in Nubia-Somalia plate motion.

In addition to exploring how the range of Red Sea opening solutions described above impacts our estimates of Nubia-Somalia plate motion, we used PDFs to approximate and propagate uncertainties in each of the six Red Sea opening rotations described above into our estimates of Nubia-Arabia plate motion. To do so, we perturbed each opening rotation with three small-angle, partial uncertainty rotations (PUR) (Stock & Molnar 1983) that we defined to isolate uncertainties in the reconstructed, margin-to-margin opening distance of the Red Sea and the reconstructed, margin-parallel component of motion. For simplicity, we assume that reconstructing a point across the Red Sea gives rise to a reconstruction uncertainty that is well approximated by a two-dimensional, 95% circular region with a radius of 2.5 km. This corresponds to a one-dimensional, 1-σ uncertainty of $\pm$1 km along great circles that are parallel and orthogonal to the Red Sea opening direction.

We constructed the probability density function for each opening rotation as follows. For each of the three PURs, we selected a trial angle randomly drawn from a Gaussian distribution centered on zero and with 1-σ values of $\pm 0.009\,^\circ$ (equivalent to a rotation error of $\pm$1 km for all points orthogonal to the PUR). We then multiplied the three small-angle PURs by the original opening rotation to find the perturbed opening rotation. Repeating the above procedure with randomly selected PUR angles gave rise to a 3-D, Gaussian-distributed cloud of trial opening rotations centered on each of the six original opening rotations. The blue symbols in Figs. S2a-f show the distributions of trial finite opening poles for all six opening-rotation PDFs. The opening-angle PDF for each of the six opening rotations (not shown) define Gaussian-distributed angles that are centered on the original opening angles.

IIb. Nubia-Arabia kinematic models

Figs. S2a-h show 10,000 samples that were randomly drawn from the opening-rotation, opening-age, and motion-change probability density functions described above. From these samples and the GPS-derived angular velocity described above, we constructed 10,000 models of Nubia-Arabia plate motion for each of the six Red Sea opening rotations described above. The derivation of the two angular velocities that comprise each model is straightforward. The angular velocity that describes motion from the present back to the time selected for the change in plate motion is by definition fixed to the GPS estimate defined above. The angular velocity for the older interval is determined by combining the trial opening rotation for the Red Sea with the trial anti-rotation for the youngest interval and then normalizing the resulting stage rotation by the time spanned by the oldest interval. For simplicity, we refer hereafter to the poles that describe motions during the younger and older intervals as the "young" and "old" poles.

The outcomes of interest from our probabilistic analysis are the range of older-interval angular velocities that satisfy the criteria described above and whether any of the models are consistent with a simple steady-opening history for the Red Sea. We discuss these in order below.

For five of the six Red Sea opening models that we explored, excepting only the Joffe & Garfunkel (1987) Red Sea opening rotation, the old poles are scattered more than 20 angular degrees to the west and northwest of the present-day GPS pole (Figs. S2a,b,d-f) and migrate progressively farther to the west as a function of the ages that are assumed for the change in motion (Fig. S2b) and for the opening of the Red Sea. By implication, the opening directions of the Red Sea as predicted by these old poles was different for the older interval than for the younger interval.

For example, representative angular velocities that are constrained to consistency with the PDF for the Sultan *et al.* (1992) Red Sea opening rotation predict that Nubia-Arabia velocities before the change in motion were faster than and clockwise from the younger-interval velocity at the northern end of the Red Sea and along the Dead Sea Fault (Fig. S3b), but predict older-interval velocities in the central Red Sea that differ insignificantly from the younger-interval velocity. At the location of the Main Ethiopian Rift, which is relevant to our study of Nubia-Somalia plate motion, the velocities for the older interval are always slower than and rotated anticlockwise (by 7-35 $^\circ$) from the younger interval velocity (Figs. S3cd and S4b).

Unlike the other old poles, the old poles that were constrained to consistency with the PDF for the Joffe & Garfunkel (1987) Red Sea opening rotation are nearly collinear with the GPS-constrained stage pole and are robust with respect to the range of Red Sea opening ages and motion-change ages that are spanned by their PDFs (compare the red symbols and open square in Fig. S2c). The opening directions predicted for the older interval are nearly the same as those predicted by the ArRajehi *et al.* (2010) GPS angular velocity everywhere along the Red Sea (Figs. S3b and S4a), as expected given the near collinearity of the old poles and the GPS pole.

Nubia-Arabia opening rates that are predicted by angular velocities for the older interval based on the Joffe & Garfunkel model are slower everywhere along the plate boundary than the younger-interval rates (Fig. S4a). An acceleration of Nubia-Arabia plate motion during the past 20 Ma is thus a robust outcome of models that are constrained to consistency with Joffe & Garfunkel's Red Sea opening rotation. In the Main Ethiopian Rift, Nubia-Arabia rates that are predicted by the older-interval angular velocities range from 7 mm yr^{-1} for trial models that assume a change in motion at 18 Ma to 17.5 mm yr^{-1} for trial models that assume a change in motion at 6 Ma (Fig. S4a). For comparison, the older-interval spreading rates predicted by angular velocities based on the Sultan *et al.* (1992) model range from 9 to 18 mm yr^{-1} at the same location (Fig. S3c). Slower

Nubia-Arabia motion at the northern end of the East Africa Rift system before 6 Ma is thus the most frequent outcome of our analysis, although some solutions are permissive of steady or nearly steady Nubia-Arabia opening rates for the past 20 Ma.

None of the numerous solutions sampled by our probabilistic analysis were permissive of steady rates and steady directions for all of the past 20 Myr, irrespective of the wide ranges of ages that are sampled by the opening-age and motion-change PDFs. We conclude that the observations and constraints that are embedded in the PDFs and the six geological models require at least one change in Nubia-Arabia plate motion during the past 20 Myr.

Overall, the Nubia-Arabia kinematic models that we derived from the Joffe & Garfunkel (1987) and Sultan *et al.* (1992) Red Sea opening rotations give the most extreme results of the six models that we tested. Since they bracket the range of likely solutions for Nubia-Arabia plate motion since 20 Ma, we next test both solutions to determine whether either is consistent with independent geological constraints.

IIc. Consistency with Dead Sea and Gulf of Suez geological constraints

During much or possibly all of the past 20 Myr, the motion between the Nubia and Arabia plates at the northern end of the Red Sea has been partitioned between the Dead Sea Fault and normal faults in the Gulf of Suez (located and labeled "DSF" and "GS" in the inset to Fig. S4) (Joffe & Garfunkel 1987). Distinctive geologic features on either side of the Dead Sea strike-slip fault have been offset sinistrally by a well-constrained 105-107 km, all during the past 20 Myr (Garfunkel, 1997; Bosworth *et al.* 2005; Garfunkel 2014). From structural, well, and seismic data, normal faults in the northern and southern Gulf of Suez are estimated to have accommodated 15 km and 36 km of extension, respectively (Bosworth & McClay 2001). Most of this extension occurred between $\sim$22 Ma and $\sim$5 Ma (Garfunkel 1997 and references therein), although extension continues to the present (Mahmoud *et al.* 2005). Additional extension was accommodated by diking, which ended by 21 Ma (Bosworth & Stockli 2016).

Freund (1970) was the first to use the geologically-estimated offsets for the Dead Sea Fault and Gulf of Suez to demonstrate that Red Sea opening models that are derived by reconstructing the Red Sea coastlines predict too much extension across the normal faults in the Gulf of Suez. Garfunkel & Beyth (2006) similarly evaluated a range of proposed Red Sea opening models to determine whether they satisfy the deformation constraints of the above features.

We use a simple three-stage procedure to evaluate whether our probabilistic estimates of Nubia-Arabia rotations based on the Joffe & Garfunkel (1987) and Sultan *et al.* (1992) Red Sea opening rotations are consistent with geologically-estimated offsets of the Dead Sea Fault and Gulf of Suez. We first used the ensembles of 10,000 Nubia-Arabia rotations associated with the two models to predict the total displacement between Nubia and Arabia across the southern Dead Sea Fault during the past 19.7 Myr. We next subtracted the 105-km geologically-constrained strike-slip offset of the N17.5 °E-striking Dead Sea Fault from each displacement vector, giving an ensemble of 10,000 residual displacement vectors per opening model (Fig. S5a). Finally, we rotated the residual displacement vectors onto N35 °W and N55 °E coordinate axes parallel and orthogonal to the rifts in the Gulf of Suez (Fig. S5b) and compared the rift-normal component to structural estimates of the cumulative extension across the Gulf of Suez (Patton *et al.* 1994; Bosworth 1995; Bosworth & McClay 2001).

The residual displacements associated with the Joffe & Garfunkel Red Sea opening rotation range from 24-54 km and have a mean direction of N07 °E (Fig. S5a), consistent with extension (as opposed to convergence) across the Gulf of Suez, but at a $\approx$50 ° angle to the N35 °W-trending

normal faults. The rift-normal component of the displacements ranges from 15 to 35 km (Fig. S5b), consistent with the 15-km and 36-km estimates of rift-normal extension in the northern and southern Gulf of Suez based on structural, well, and seismic data (Bosworth & McClay 2001). We conclude that Nubia-Arabia kinematic models based on Joffe & Garfunkel's (1987) Red Sea opening rotation satisfy the geological constraints on offsets across the Dead Sea Fault and faults in the Gulf of Suez within the bounds of the PDFs embedded in our probabilistic analysis.

The residual displacements associated with the Sultan *et al.* Red Sea opening rotation range from 59-89 km and have a mean direction of N33 °E (red circles in Fig. S5a). The residual displacements are thus larger than and less oblique to the normal faults than for the Joffe & Garfunkel model. The rift-normal components of the displacements range from 48 to 81 km (red circles in Fig. S5b), larger than 15-36 km structural estimates. The Sultan *et al.* Red Sea opening rotation is thus inconsistent with the structurally-derived offsets for the Dead Sea Fault and faults in the Gulf of Suez, irrespective of the range of parameters that are sampled by our probabilistic analysis. Our results concur with conclusions previously reached by Garfunkel & Beyth (2006) about the incompatibility of the Sultan *et al.* (1992) Red Sea opening rotation with the geological constraints at the northern end of the Red Sea.

Based on these results, the ensemble of Nubia-Arabia rotations that are derived from the Joffe & Garfunkel model appears to be the stronger basis for our ensuing estimates of Nubia-Somalia plate motion. In the main document, we thus use Nubia-Arabia rotations that are based (in part) on the Joffe & Garfunkel (1987) Red Sea opening rotation as our basis for estimating bounds on motion between Nubia and Somalia.

Table 1: Nubia-Somalia best-fitting rotations from Southwest Indian Ridge

Chron	Lat.	Long.	Ω	Covariances					
	(°N)	(°E)	(degrees)	a	b	c	d	e	f
1n	-39.73	6.75	0.029	18.1	-7.0	-7.1	7.1	-1.3	9.5
2n	-40.39	9.44	0.065	90.4	64.6	-128.7	94.4	-92.8	255.4
2An.1	-47.56	15.37	0.150	76.8	40.3	-86.3	61.0	-42.7	195.2
2An.3	-49.76	12.29	0.227	178.6	78.3	-208.4	90.0	-104.5	398.9
3n.1	-49.54	10.08	0.265	254.7	132.3	-283.5	172.8	-145.7	580.9
3n.4	-49.88	354.47	0.237	290.3	113.9	-334.5	159.8	-208.2	689.3
3An.1	-47.79	353.20	0.215	247.7	94.4	-305.7	159.7	-188.4	615.1
3An.2	-42.36	347.48	0.187	350.4	146.4	-443.1	236.0	-280.1	824.8
4n.1	-45.95	14.23	0.341	480.0	240.8	-585.3	313.7	-372.8	920.4
4n.2	-45.39	359.23	0.250	499.6	180.6	-593.3	255.6	-327.9	1014.9
4A	-46.35	12.01	0.432	765.6	164.6	-757.8	243.0	-355.3	1063.0
5n.1	-41.18	17.58	0.493	946.8	366.8	-979.1	282.3	-491.9	1262.6
5n.2	-42.10	10.04	0.432	277.3	80.5	-320.6	73.0	-131.3	530.2
5An.2	-43.86	3.59	0.443	355.7	116.9	-410.5	138.6	-202.2	719.1
5AC	-45.14	3.07	0.586	302.4	116.7	-276.2	196.3	-215.8	613.2
5AD	-45.11	9.11	0.670	488.7	272.3	-536.2	492.9	-500.8	993.4
5Cn.1	-47.00	12.51	0.882	2438.6	569.2	-2563.4	546.4	-1111.5	3878.6
6ny	-42.04	16.03	1.090	5210.8	434.2	-3140.9	407.4	-413.3	2588.3
6no	-33.21	6.53	0.644	765.9	321.8	-405.5	515.4	-122.6	774.0

These rotations reconstruct movement of the Somalia plate relative to the Nubia plate and are determined from combining Nubia-Antarctica and Somalia-Antarctica rotations from Tables 2 and 4 of DeMets *et al.* (2015). Rotation angles Ω are positive anticlockwise. The Cartesian rotation covariances are calculated in a Somalia-fixed reference frame and have units of 10^{-9} radians^2. Elements *a*, *d*, and *f* are the variances of the (0 °N, 0 °E), (0 °N, 90 °E), and 90 °N components of the rotation. See the footnotes for Table 1 of the main document for instructions on how to rebuild the covariance matrix.

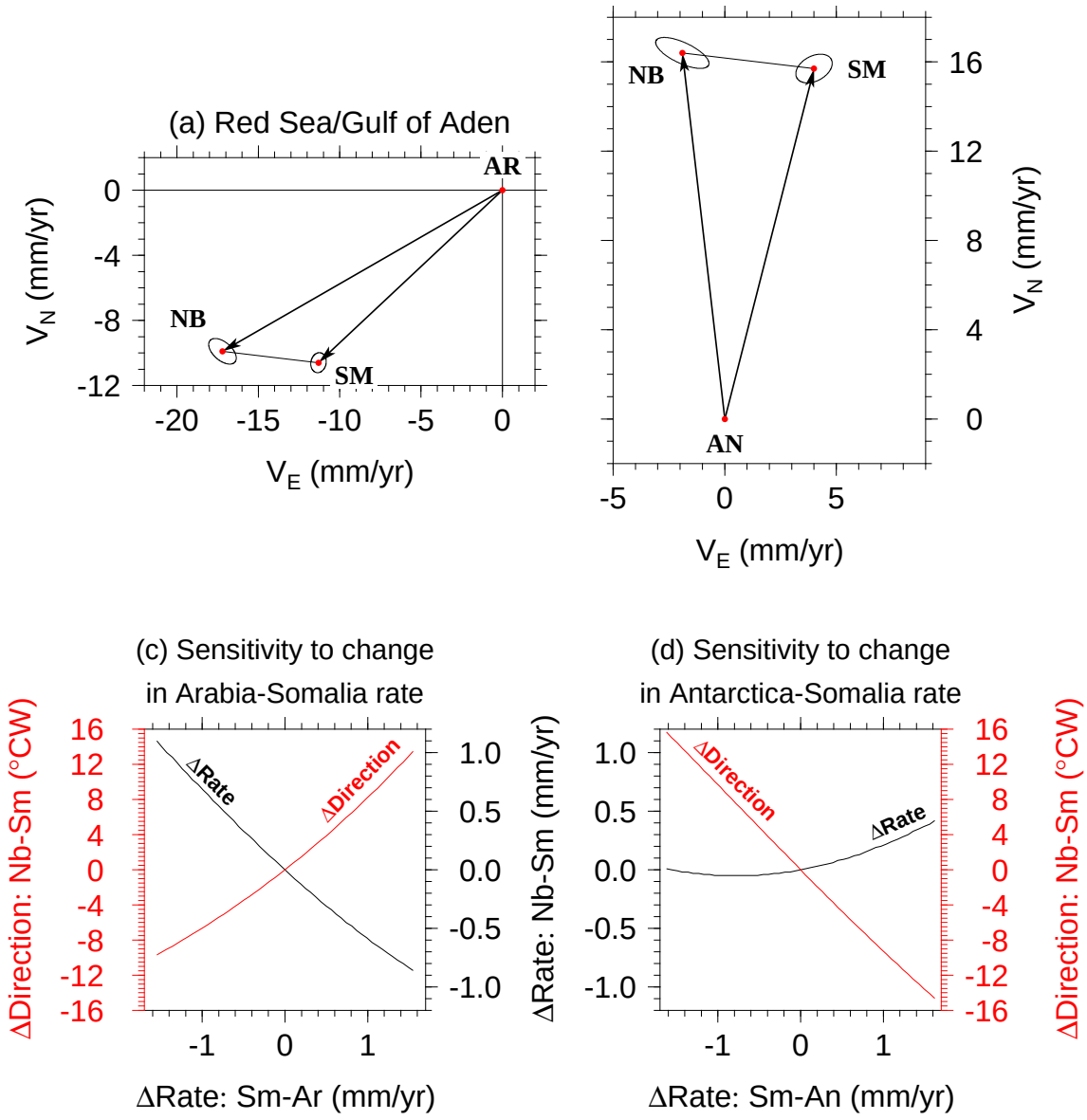

Fig. S1. Linear velocities for the Nubia-Arabia-Somalia (a) and Nubia-Antarctica-Somalia (b) plate circuits estimated at 9 °N, 40 °E from the 3.16-Myr-average MORVEL angular velocities (DeMets *et al.* 2010). (c) Trade-off between speed-ups or slowdowns in the Arabia-Somalia rate and the Nubia-Somalia velocity magnitude and orientation at 9 °N, 40 °E. Changes of only ±1 mm/yr in the Arabia-Somalia rate (horizontal axis) cause changes as large as 10 ° in the Nubia-Somalia direction (red line) when closure of the velocity circuit shown in (a) is enforced. To first-order, the same tradeoffs exist for changes in the Arabia-Nubia rate. (d) Sensitivities of the predicted Nubia-Somalia rate and direction to small speed-ups or slowdowns in the Antarctica-Somalia rate. Nearly the same tradeoffs exist for changes in the Antarctica-Nubia rate. For the Nubia-Antarctica-Somalia plate circuit, the estimated Nubia-Somalia rate is relatively insensitive to errors in the estimated Nubia-Antarctica or Somalia-Antarctica rates.

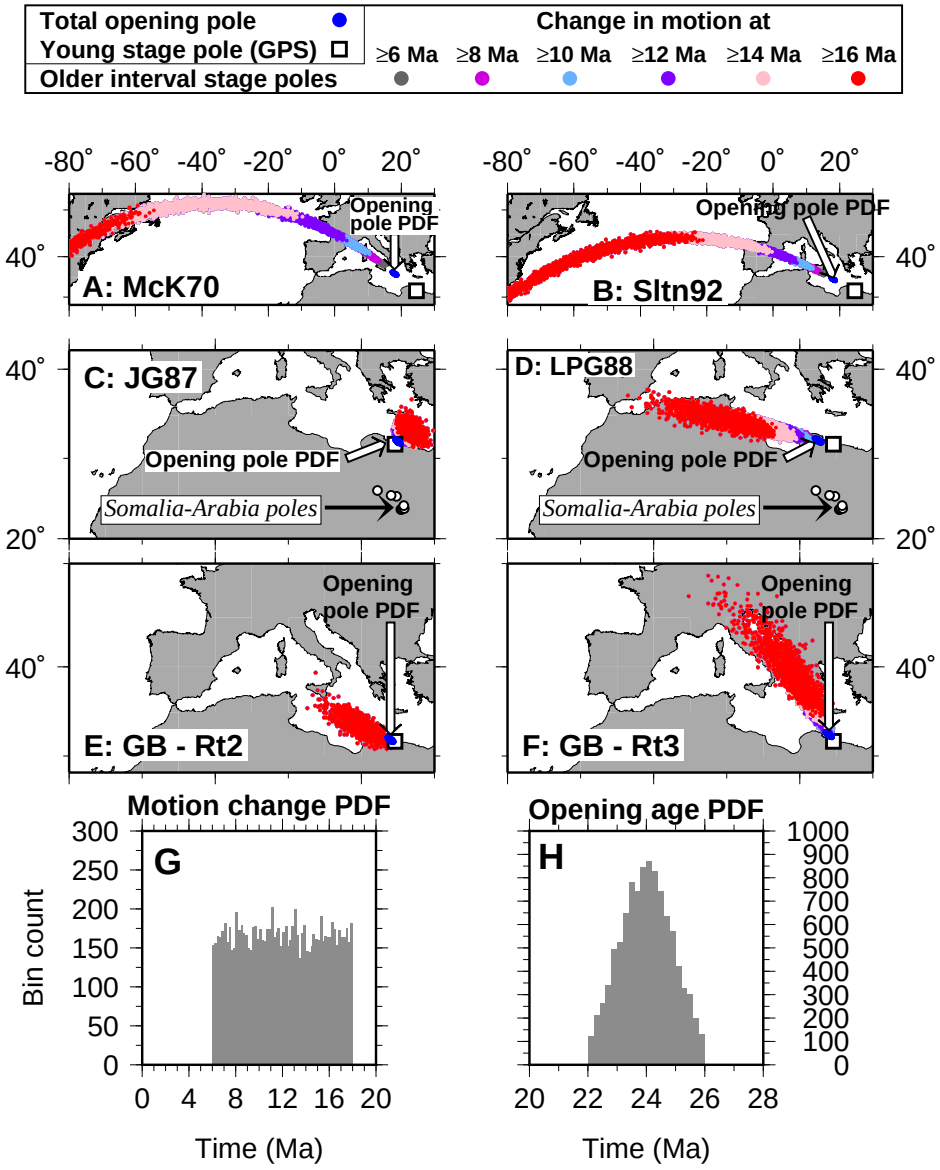

Fig. S2. Probability density functions (PDF) used to construct trial models for the history of Nubia-Arabia (Nb-Ar) motion across the Red Sea. (a-f) Present-day (GPS), total-opening, and stage poles that constrain Red Sea opening per model tested. Open square locates the GPS pole of ArRajehi *et al.* (2010). Blue symbols show total opening pole estimates, with abbreviations as follows: ”McK70” - McKenzie *et al.* (1970); ”Sltn92” - Sultan *et al.* (1992); ”JG87” - Joffe & Garfunkel (1987); ”LPG88” - Le Pichon & Gaulier (1988); ”GB-Rt2” and ”GB-Rt3” from Table 3 of Garfunkel & Beyth (2006). Red circles show Nubia-Arabia stage poles that describe opening from the time that the Red Sea opened until the time that motion is assumed to have changed (see text). Arabia-Somalia poles from Table 3 are shown in (c) and (d). The methods used to determine the acceptable (Gaussian) limits on the total opening poles (and opening angles, which are not shown), are described in the text. (g) Distribution of ages at which Nubia-Arabia plate motion is assumed to have changed. These are limited to ages between 6 and 18 Ma. (h) Distribution of ages at which opening of the Red Sea is assumed to have occurred. These are limited to ages between 22 and 26 Ma. Results for ten thousand independent trial estimates for each of the above models are shown.

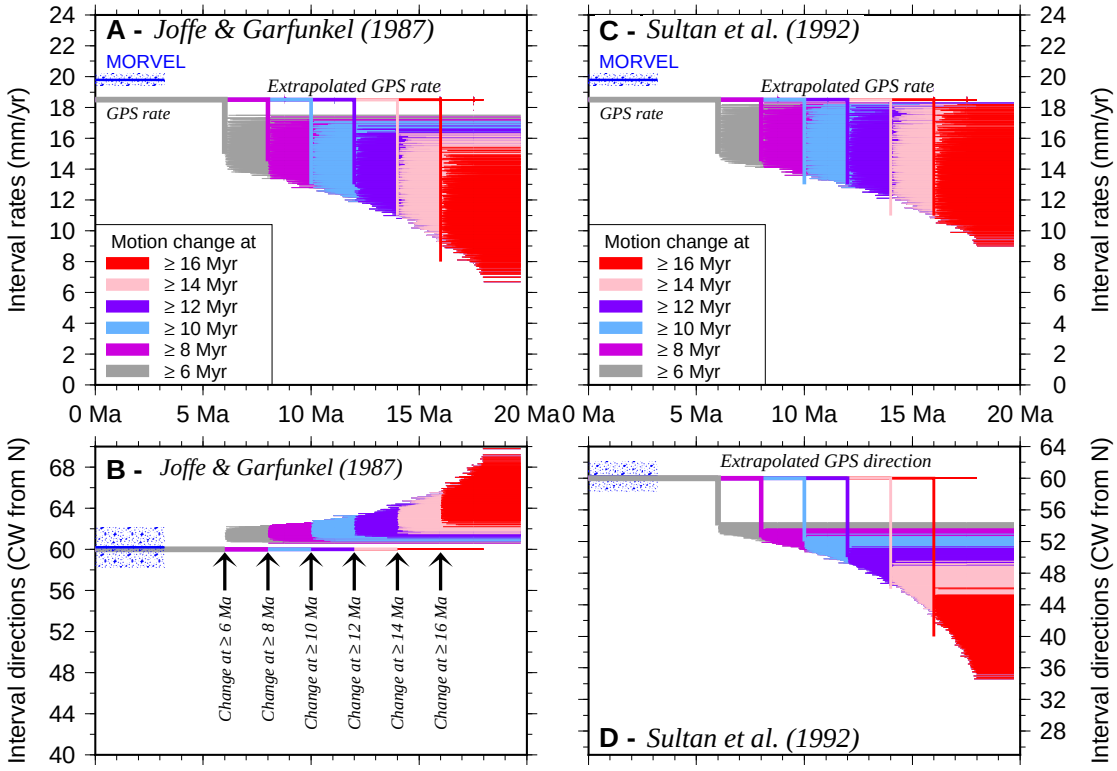

Fig. S3. Nubia-Arabia opening rates (a & c) and directions (b & d) based on Red Sea opening rotations estimated by Joffe & Garfunkel (1987) and Sultan *et al.* (1992). The estimates based on these two models are end-member results amongst the six published models described in the text and shown in Fig. S2a-f. Estimates of Nubia-Arabia plate motion are derived by assuming two intervals of constant plate motion since the Red Sea opened. As described in the text, motion during the younger interval is defined by a rotation that is extrapolated from GPS (see text) and motion during the older interval is defined by a stage rotation that is estimated from the difference between the younger rotation and the assumed total opening rotation for the Red Sea. The age when Nubia-Arabia motion changed and the age that opening commenced across the Red Sea are treated as unknowns and are drawn from probability distribution functions shown in Fig. S2gh. Results from 10,000 trial models are illustrated. Velocities are calculated at 9.0 °N, 40.0 °E.

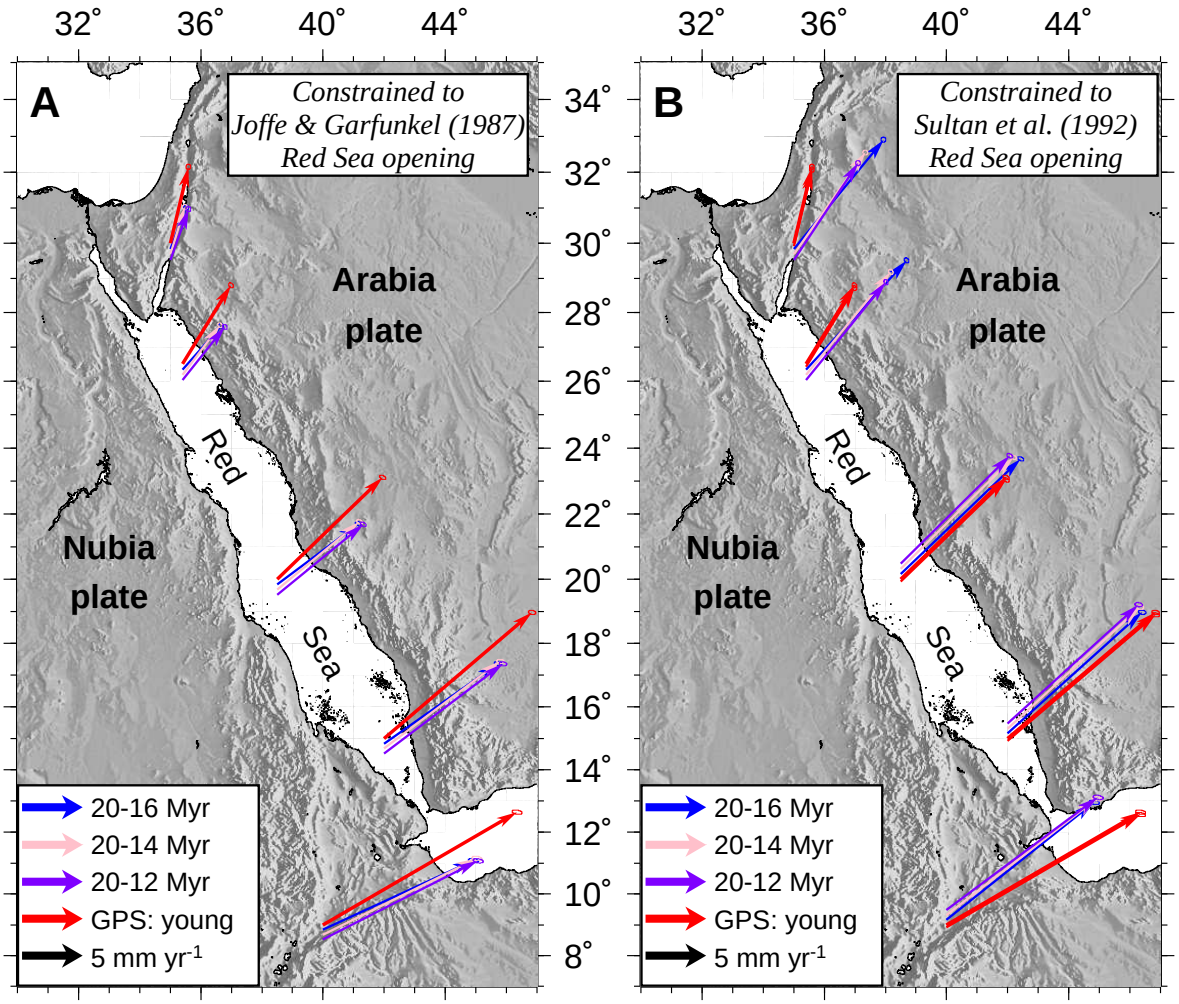

Fig. S4. Comparison of Nubia-Arabia velocities between the Dead Sea Fault in the north and Main Ethiopian Rift in the south as predicted by the older-interval and younger-interval angular velocities determined from the probabilistic analysis described in Section 3 of the main document. The velocities labeled ”GPS” in both panels are predicted by the GPS-derived Nubia-Arabia angular velocity of ArRajehi *et al.* (2010), which is assumed to be representative of Nubia-Arabia motion during the younger (recent) interval. The older-interval velocities, variously labeled ”20-16 Myr”, etc, assume that opening of the Red Sea started at 24 Ma and that plate motion variously changed at 12 Myr, 14 Myr, or 16 Myr. The older-interval rotations in Panels A and B are constrained to consistency with the Joffe & Garfunkel (1987) and Sultan *et al.* (1992) Red Sea opening rotations, respectively.

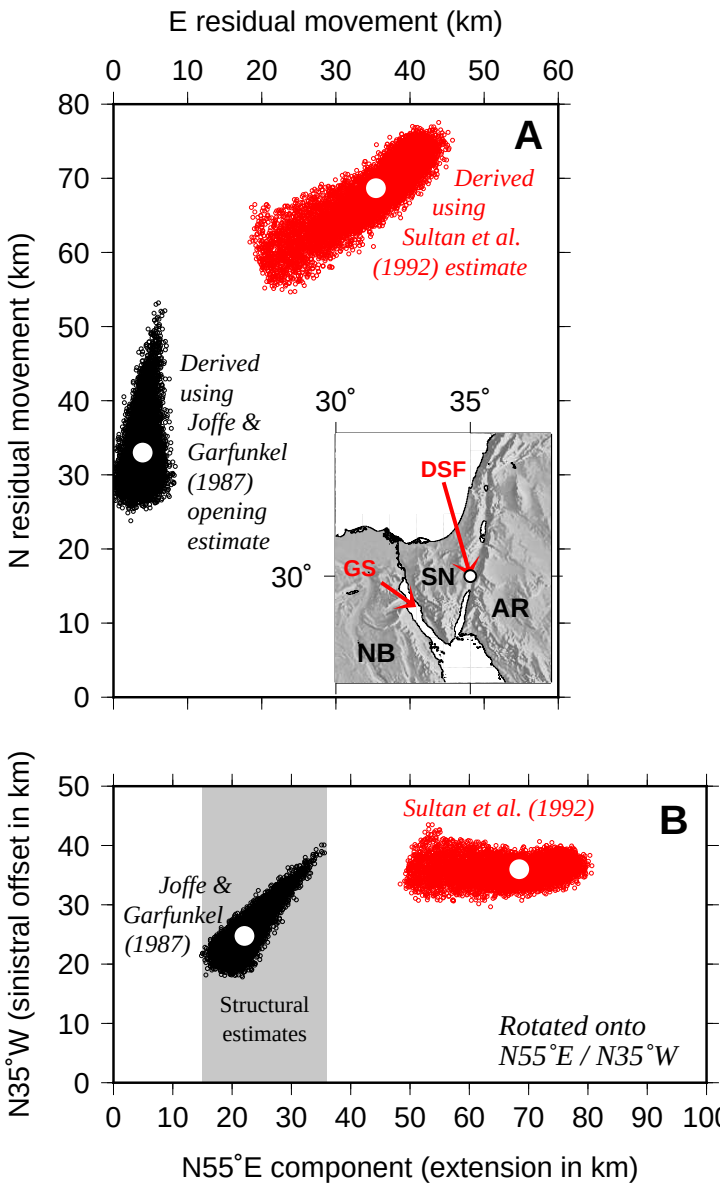

Fig. S5. Test of end-member Red Sea (Nubia-Arabia) opening models against geological slip estimates for the Dead Sea Fault and normal faults in the Gulf of Suez (labeled ”DSF” and ”GS” respectively in the inset map). Panel A shows the predicted displacement of Nubia relative to the Arabia plate at 19.7 Ma reduced by 105 km of post-20-Myr left-lateral slip along the N17.5 °E-trending Dead Sea Fault (Garfunkel 2014). The Nubia-Arabia displacements are predicted at a location along the Dead Sea Fault using probabilistic estimates based on the Joffe & Garfunkel (1987) and Sultan *et al.* (1992) estimates (see text). The residual movement shown in Panel A was presumably accommodated partly or wholly by normal faulting across the Gulf of Suez. Open circles show the average of each distribution. In Panel B, the residual movements from Panel A are rotated onto axes that trend N55 °E and N35 °W, which are orthogonal and parallel to the trend of normal faults in and along the Gulf of Suez. The gray area shows 15-36 km structural estimates of the total extension across normal faults in the northern and southern Gulf of Suez (Bosworth & McClay 2001). Abbreviations: AR, Arabia plate; NB, Nubia plate; SN, Sinai microplate.

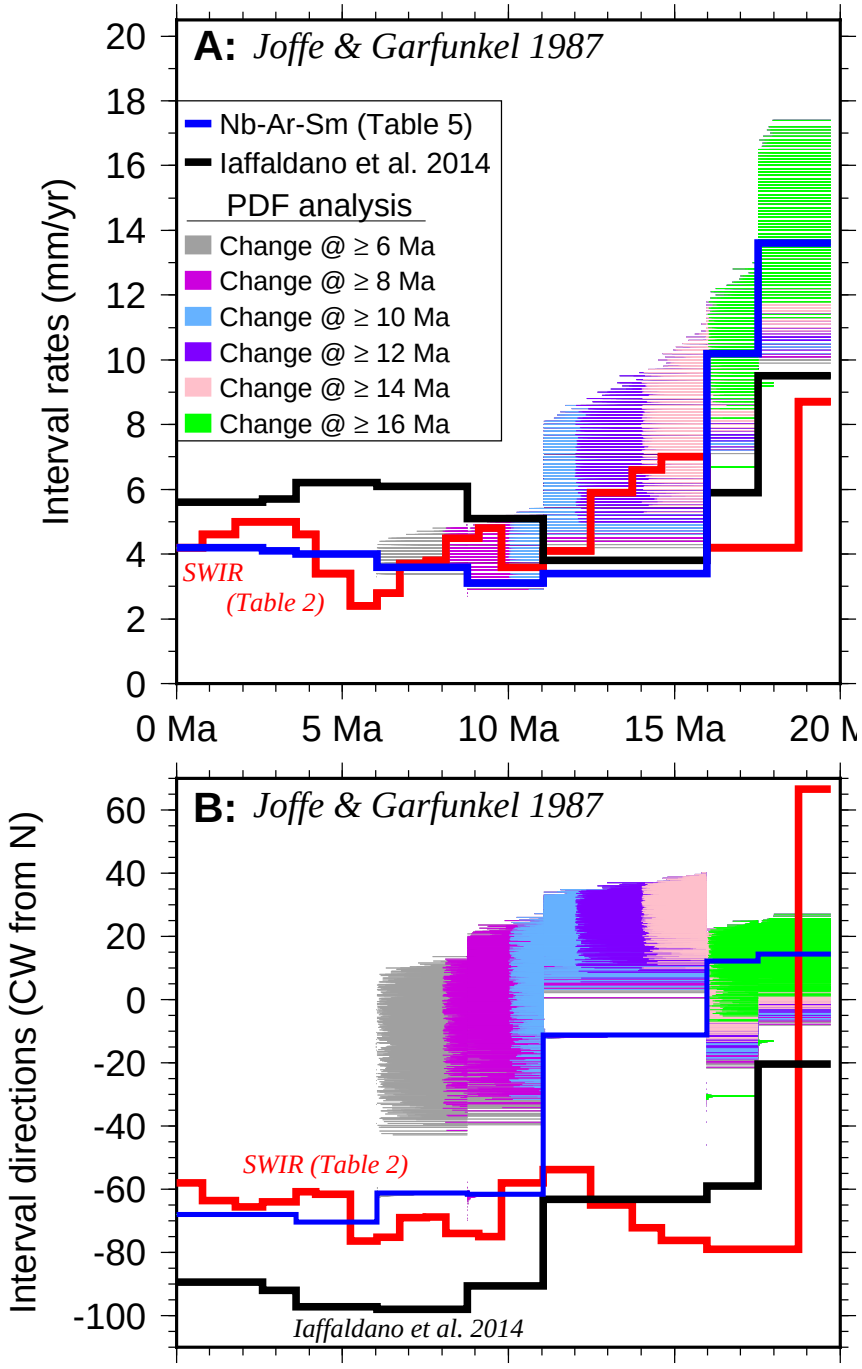

Fig. S6. Motion of Nubia relative to Somalia plate, 20 Ma to present. (a) and (c) show interval rates and (b) and (d) show interval directions that are predicted at 9.0 °N, 40.0 °E by stage rotations determined from the rotations in Tables 1 and 4, from our probability-density-function (PDF) analysis, and from Iaffaldano *et al.* (2014). Stage rotations labeled "SWIR" are determined from the finite rotations in Table 1 of the main document, which are based on reconstructions of data from the Southwest Indian Ridge (SWIR). Stage rotations from the latter three sources are determined from finite rotations that reconstruct data from the Gulf of Aden and Red Sea. Gray and other colored regions show the range of interval velocities derived by combining the Somalia-Arabia noise-reduced rotations in Table 3 with ten thousand Nubia-Arabia trial rotations that were derived from the probability density function (PDF) analysis described in the text. Probabilistic velocity estimates are propagated from the Joffe & Garfunkel (1987) Red Sea (Nubia-Arabia) opening rotation.

References not included in the citation list for the main document

Almaki, K. A., Betts, P. G., & Ailleres, L., 2014. Episodic sea-floor spreading in the southern Red Sea, *Tectonophys.*, **617**, 140–149.

Bosworth, W., 1995. A high-strain rift model for the southern Gulf of Suez (Egypt), in *Hydrocarbon habitat in rift basins, Spec. Pub. - Geol. Soc. London*, ed. Lambiase, J. J., **80**, 75–112.

Bosworth, W. B., & Stockli, D. F., 2016. Early magmatism in the greater Red Sea rift: timing and significance, *Canadian J. Earth Sci.*, 10.1139/cjes–2016-0019.

Bosworth, W., & McClay, K., 2001. Structural and stratigraphic evolution of the Gulf of Suez Rift, Egypt: A Synthesis, in *Peri-Tethys Memoir 6: Peri-Tethyan Rift/Wrench Basins and Passive Margins, Mem. Mus. natn. Hist. nat.*, **186**, 567–606, eds. P. A. Ziegler, E W. Cavazza, A. H. F. Robertson, and S. Crasquin-Soleau, Paris.

Chu, D., & Gordon, R. G., 1998. Current plate motions across the Red Sea, *Geophys. J. Int.*, **135**, 313–328.

DeMets, C., Merkouriev, S., & Sauter, D., 2015. High-resolution estimates of Southwest Indian Ridge plate motions, 20 Ma to present, *Geophys. J. Int.*, **203**, 1495–1527.

Dyment, J., Tapponnier, P., Affi, A. M., Zinger, M. A., Franken, D., & Muzaiyen, E., 2013. A new seafloor spreading model of the Red Sea: magnetic anomalies and plate kinematics, abstract T21A-2512 presented at the 2013 Fall Meeting, AGU, San Francisco, Calif., 9-13 Dec.

Garfunkel, Z., 1997. The history and formation of the Dead Sea Basin, in *The Dead Sea: The Lake and Its Settings*, 36–56, eds. Niemi, T. M., Ben-Avraham, Z., and Gat, J. R., Oxford University Press, Oxford.

Garfunkel, Z., 2014. Lateral motion and deformation along the Dead Sea transform, in *Dead Sea Transform Fault System: Reviews*, Modern Approaches in Solid Earth Sciences, 109–150, eds. Garfunkel, Z., Ben-Avraham, Z., & Kagan, E., Springer, London.

Lazar, M., Ben-Avraham, Z., & Garfunkel, Z., 2012. The Red Sea - New insights from recent geophysical studies and the connection to the Dead Sea fault, *J. Afr. Earth Sci.*, **68**, 96–110.

Le Pichon, X., & Gaulier, J.-M., 1988. The rotation of Arabia and the Levant fault system, *Tectonophys.*, **153**, 271–294.

Mahmoud, S., Reilinger, R., McClusky, S., Vernant, P., & Tealeb, A., 2005. GPS evidence for northward motion of the Sinai Block: Implications for E. Mediterranean tectonics, *Earth Planet. Sci. Lett.*, **238**,217–224.

Merkouriev, S., & DeMets, C., 2006. Constraints on Indian plate motion since 20 Ma from dense Russian magnetic data: Implications for Indian plate dynamics, *Geochem. Geophys. Geosyst.*, **7, Q02002**, doi:10.1029/2005GC001079.

Mitchell, N. C., & Park, Y., 2014. Nature of crust in the central Red Sea, *Tectonophys.*, **628**, 123–139.

Patton, T. L., Moustafa, A. R., Nelson, R. A., & Abdine, S. A., 1994. Tectonic evolution and structural setting of the Suez Rift, in *Interior Rift Basins*, ed. Landon, S. M., *AAPG Memoir*, **59**, 7–55.

Stock, J. M., & Molnar, P., 1983. Some geometrical aspects of uncertainties in combined plate reconstructions, *Geology*, **11**, 697–701.

Sultan, M., Becker, R., Arvidson, R. E., Shore, P., Stern, R. J., El Alfy, Z., & Attia, R. I., 1993. New constraints on Red Sea rifting from correlations of Arabian and Nubian Neoproterozoic outcrops, *Tectonics,* **12**, 1303–1319.

Tapponnier, P., Dyment, J., Zinger, M. A., Franken, D., Affi, A. M., Wyllie, A., Ali, H. G., & Hanbal, I., 2013. Revisiting seafloor-spreading in the Red Sea: Basement nature, transforms, and ocean-continent boundary, abstract T12B-04 presented at the 2013 Fall Meeting, AGU, San Francisco, Calif., 9-13 Dec.